

Electrophilic and radical reactivity of ionized aminohydroxycarbene toward alkenes

Guy Bouchoux*, Julia Chamot-Rooke

Laboratoire des Mécanismes Réactionnels, UMR CNRS 7651, Ecole Polytechnique, F-91128 Palaiseau Cedex, France

Received 19 February 2002; accepted 26 March 2002

Abstract

Ion molecule reactions between ionized aminohydroxycarbene, $[\text{NH}_2\text{COH}]^{\bullet+}$, **1**, and several representative alkenes (ethene, propene, 1-butene, 2-butene) were studied by Fourier transform ion cyclotron resonance mass spectrometry. Condensation processes were evidenced by the fragmentation pattern of the elusive collision complex which exhibits the characteristic behavior of the corresponding ionized aliphatic amide. Mechanistic pathways, corroborated by collision induced dissociation and deuterium labeling experiments and by G2 molecular orbital calculations, are proposed to explain the observed pattern. Proton and hydrogen atom transfer were also detected in several cases. (Int J Mass Spectrom 219 (2002) 625–641)
© 2002 Elsevier Science B.V. All rights reserved.

Keywords: Carbene ions; Condensation reaction; Hydrogen atom and proton transfers; G2 calculations

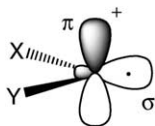
1. Introduction

Twenty years ago, Hoppilliard et al. [1] investigated the keto–enol tautomerism of several radical cations by use of the MINDO/3 semi-empirical method of quantum chemistry. The main conclusion of this study was that the energetically favored pathway from ionized aldehydes to their enol form is a two step process involving the corresponding ionized carbene. Although it rapidly appears that MINDO/3 seriously overestimate the stability of ionized carbenes, the involvement of these latter species during isomerization of ionized carbonylated molecules has been further corroborated. It has been, for example, established that ionized acetaldehyde may

isomerize to ionized vinylalcohol by two successive 1,2-hydrogen shifts thus passing through the hydroxymethyl carbene structure [2]. During the years, the identification of ionized carbenes in the gas phase and the understanding of their chemistry has significantly advanced (for a recent review on ionized carbenes, see [3]). However, most of this interest has been limited to their unimolecular chemistry. By contrast, our knowledge of the bimolecular chemistry of ionized carbenes is poorly documented despite of their unique ability to induce both cationic and radical reactivity on the same carbon atom. It is the goal of the present study to bring informations on the peculiar ion–molecule chemistry of a well characterized ionized carbene: ionized aminohydroxycarbene $[\text{NH}_2\text{COH}]^{\bullet+}$, **1**.

The electronic structure of an ionized carbene, in its ground state, is of the type σ^{\bullet}/π^+ :

* Corresponding author.
E-mail: bouchoux@dcmr.polytechnique.fr



It is therefore expected that $XYZ\bullet^+$ radical cations should be stabilized by π -donor substituents X and Y. Accordingly most of the presently identified ionized carbenes correspond to a carbenic center bearing unsaturated hydrocarbon moiety or heteroatoms such as fluorine, oxygen or nitrogen [3]. Moreover, the stabilizing effect of the substituent X or Y may render the ionized carbene much more stable than its conventional isomers. This situation is particularly anticipated for nitrogen substituted carbenes owing to the well known donor ability of this element. Recently, we found, by quantum chemical calculations at the G2(MP2,SVP) level, that ionized aminohydroxycarbene $[NH_2COH]\bullet^+$, **1**, is the global minimum of the potential energy surface of the $[N,C,O,H_3]\bullet^+$ system [4]. Moreover, this structure is protected against isomerization and dissociation by energy barriers higher than 170 kJ/mol. This explains why its experimental characterization has been possible [5] and thus prompted us to explore its bimolecular reactivity.

2. Methods

Ionized aminohydroxycarbene may be obtained by electron dissociation of methyl carbamate, oxamic acid, oxamide or propionamide [5]. We find that the higher yield of $[N,C,O,H_3]\bullet^+$ ions was obtained when using oxamide as precursor molecule in our experimental conditions. All reactions were monitored in a Bruker CMS 47-X ion cyclotron resonance mass spectrometer equipped with an external ion source [6]. Experiments consist of transferring all the ions resulting from electron ionization of oxamide to the reaction cell located inside the 4.7 T superconducting magnet. The ions m/z 45, $[C,O,N,H_3]\bullet^+$ are then selected by ejection of unwanted ionic species by a combination of soft and chirp rf pulses. After selection, the reactant ions are relaxed to thermal energy

by introducing argon inside the reaction cell and by imposing a suitable relaxation delay (typically 2 s). Next, the ions were allowed to react for a variable time with neutral molecules M at a pressure in the range 10^{-8} to 2×10^{-8} mbar. The characterization of the most significant product ions has been done by means of low energy collision induced dissociation in the FT-ICR cell. Their elemental compositions have been obtained in the high resolution mode. The bimolecular rate constants k_{exp} were deduced from the slope of the logarithmic plot of the abundance of reactant ions vs. reaction time. The estimated error on the experimental rate constant values is ca. $\pm 10\%$. The collision rate constants, k_{coll} were calculated using the trajectory calculations developed by Su and Chesnavich [7].

The mass analyzed ion kinetic energy (MIKE) spectra have been obtained by scanning the electrostatic sector voltage of a BE VG-Micromass ZAB-2F mass spectrometer, after selection of the precursor ions.

The chemical samples used during our experiments were of research grade and purchased from Aldrich Chemical (GB) or Messer Griesheim GmbH (Germany).

All ab initio quantum chemical calculations were performed by using the Gaussian 98 set of programs [8]. It has been established that accurate energies (i.e., ± 5 kJ/mol) can be obtained from calculations at the G2 level of theory or its variants G2(MP2) and G2(MP2,SVP) [9,10]. For the present investigation, we utilized the G2 technique. Heats of formation were deduced from the G2 total energy by using a thermodynamic cycle involving the atomization reaction of the species considered [11]. The 0 K heat of formation of **X** is simply given by

$$\Delta_f H^\circ(\mathbf{X}, 0 \text{ K}) = E[\text{G2}](\mathbf{X}) + \sum \Delta_f H^\circ(\text{atoms}, 0 \text{ K}) - \sum E[\text{G2}](\text{atoms})$$

and, at 298 K, by

$$\Delta_f H^\circ(\mathbf{X}, 298 \text{ K}) = \Delta_f H^\circ(\mathbf{X}, 0 \text{ K}) + \int C_p(\mathbf{X}) dT - \sum \int C_p(\text{elements}) dT$$

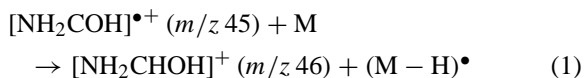
with

$$\int C_p(\mathbf{X}) dT = H^\circ(\mathbf{X}, 298 \text{ K}) - H^\circ(\mathbf{X}, 0 \text{ K})$$

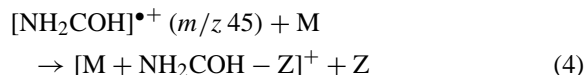
This procedure has been applied to several ionic and neutral structures for which no experimental heat of formation was available, the results are gathered in [Appendix A](#).

3. Results and discussion

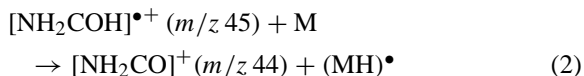
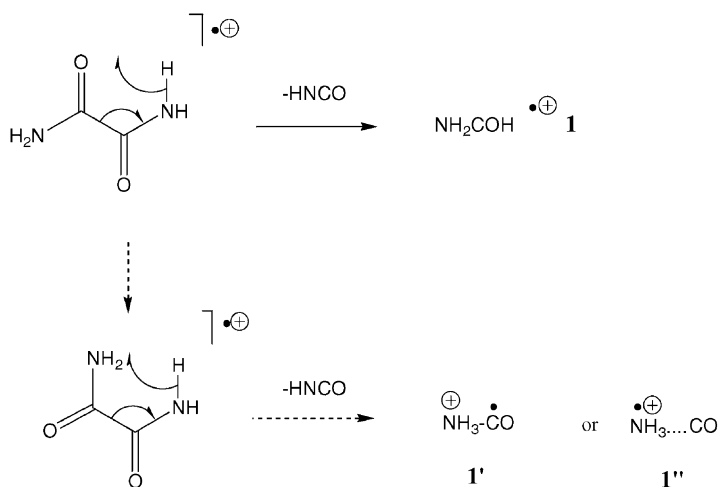
Ionized aminohydroxycarbene $[\text{NH}_2\text{COH}]^{\bullet+}$, **1**, has been allowed to react with several alkenes **M** (**M** = ethene, **2**; propene, **3**; 2-butene, **4**; and 1-butene, **5**) in the FT-ICR cell. The ionic products detected correspond to hydrogen atom transfer products (ions m/z 46 and 44, reactions (1) and (2)):



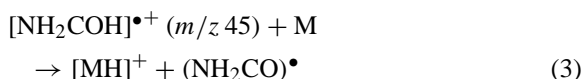
the condensation products (ions $[\text{M} + \text{NH}_2\text{COH} - \text{Z}]^+$, reaction (4)):



No significant charge exchange reaction is expected due to the low ionization energy value of the neutral aminohydroxycarbene (the adiabatic ionization energy of the singlet NH_2COH calculated at the G2 level is 8.44 eV). However, in several cases, a small signal corresponding to $\text{M}^{\bullet+}$ is detected, this may be attributed to a small amount of m/z 45 ions of a structure different from **1**. Accordingly, molecular orbital calculations [4] indicate that ions $[\text{NH}_3\text{CO}]^{\bullet+}$ resulting in a covalent bond (**1'**) or a complex (**1''**) between ionized ammonia and carbon monoxide are only slightly less stable than **1**. These two species may be competitively produced from ionized oxamide:



to proton transfer products (ions $[\text{MH}]^+$, reaction (3)):



and to fragment ions originating from losses of a neutral moiety **Z** (**Z** = H^\bullet , NH_2^\bullet , alkyl $^\bullet$, alkene) from

The recombination energy of such ions (i.e., the reverse of the ionization energy of the corresponding neutral) may be estimated to ~ 9.9 eV and, in such circumstance, charge exchange with **M** becomes possible, as observed for 1-butene and 2-butene. The possible participation of ions **1'** and **1''** to the bimolecular chemistry seems however strictly limited to these marginal charge exchange processes.

Table 1

Ions abundancies at half reaction time for the reaction of **1** with various alkenes, M^a

M	Reaction (1)		Reaction (2)		Reaction (3)		Condensation			Charge exchange	
	<i>m/z</i> 46 (%)	ΔH°	<i>m/z</i> 44 (%)	ΔH°	MH ⁺ (%)	PA[M] ^b	<i>m/z</i>	Z	%	%	IE[M] ^c
Ethene 2	8	−60	50	−28	4	680	72	H•	18	4	10.51
							57	NH ₂ •	16		
Propene 3	25	−122	0	−27	13	752	86	H•	4	0	9.73
							72	CH ₃ •	45		
							59	C ₂ H ₄	13		
2-Butene 4	20	−128	27	−12	15	747	86	CH ₃ •	22	6	9.13
							73	C ₂ H ₄	10		
1-Butene 5	21	−140	6	−24	15	735	86	CH ₃ •	14	6	9.55
							73	C ₂ H ₄	13		
							72	C ₂ H ₅ •	21		
							59	C ₃ H ₆	4		

^aExperimental relative uncertainty is about several % except for reaction (2) where it attains ca. $\pm 20\%$.^bProton affinity of the alkene M [18].^cAdiabatic ionization energy of the alkene M [19].

Table 1 summarizes the product ions abundance measured for reactions between **1** and M = **2–5**, and some of the relevant thermochemical information. As an example, Fig. 1 presents the evolution of the ion abundances as a function of the reaction time for the ethene molecule, **2**.

An important point to note is the high efficiency of the studied reactions. The reaction efficiency, defined by the ratio $k_{\text{exp}}/k_{\text{coll}}$, where k_{coll} is the collision rate coefficient, range from 50% for ethene to ca. 100%

for 2-butene. Intermediate values of 75% are obtained for propene and 1-butene. A detailed examination of each reaction route and of their possible mechanisms will be examined in the following sections.

3.1. Hydrogen atom and proton transfers

Reactions (1), (2) and (3) are under the dependence of the hydrogen atom affinity of ions $[\text{NH}_2\text{COH}]^{\bullet+}$ and $[\text{NH}_2\text{CO}]^+$ and the proton affinity of the radical

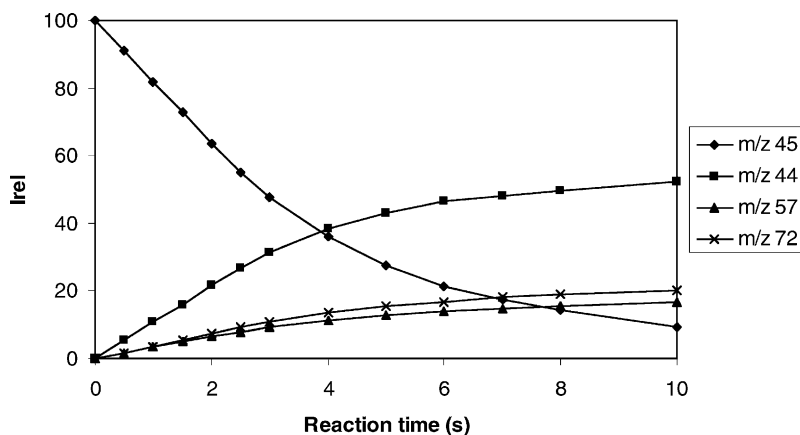
Fig. 1. Normalized peak intensities vs. time for the reaction of **1** with ethene **2** ($P = 1.6 \times 10^{-8}$ mbar).

Table 2

G2 calculated total energies (Hartree) and heats of formation (kJ/mol) for aminohydroxycarbene and its H variants

Species	E_0 K	$\Delta_f H_0$ K	$\Delta_f H_{298}$ K
$[\text{NH}_2\text{COH}]^{\bullet+}$, 1	−169.275678	786.9	776.6
NH_2COH (neutral)	−169.585960	−27.6	−38.1
$[\text{NH}_2\text{CHOH}]^{\bullet+}$	−169.960248	518.4	503.5
$[\text{NH}_2\text{CO}]^+$	−168.730081	690.6	684.1
$[\text{NH}_2\text{CO}]^{\bullet}$	−168.996245	−8.1	−13.7

$(\text{NH}_2\text{CO})^{\bullet}$, respectively. These quantities were not available and we have thus estimated their values by ab initio molecular orbital calculations at the G2 level. Table 2 lists the G2 calculated total energies and the corresponding heats of formations obtained using the “atomization” procedure described in the computational section.

Considering these data, the hydrogen atom affinity of the ions $[\text{NH}_2\text{COH}]^{\bullet+}$ and $[\text{NH}_2\text{CO}]^+$ are equal to 491.1 and 125.5 kJ/mol, respectively, the proton affinity of the radical $(\text{NH}_2\text{CO})^{\bullet}$ is calculated to be 739.7 kJ/mol (using $\Delta_f H^\circ[\text{H}]^+ = 1530$ kJ/mol [19]).

Hydrogen atom abstraction by the carbenic center of **1** to produce ions m/z 46 (reaction (1)) is not always observed, despite a favorable enthalpy of reaction (Table 1). In fact, peaks at m/z 46 are only noticeable for **M** = **3**, **4** and **5**, i.e., when an allylic radical is simultaneously produced. In those cases, reaction (1) is exothermic by more than 120 kJ/mol, by contrast, for **M** = **2** the exothermicity is equal to 60 kJ/mol. These observations suggest that the hydrogen atom transfer needs a significant activation barrier which may be erased by the stabilization of the products. A double well potential energy profile may account for this phenomenon. In a first step, reaction (1) provides an encounter complex stabilized by intermolecular (probably electrostatic) interactions, then the hydrogen transfer may occur with a critical energy E_0 to give a second complex involving, that time, the future products. According to the Bell–Evans–Polanyi principle [15], the critical energy E_0 is related to the reaction enthalpy and to the intrinsic energy barrier E_{0i} by a relationship of the type $E_0 = E_{0i} + \alpha \Delta H^\circ$. For intermolecular hydrogen atom transfers between

free radicals, intrinsic barriers are typically close to ca. 60 kJ/mol [16], consequently, for exothermic reactions, E_0 will be less than this value. Moreover, if E_0 becomes lower than the stabilization energy of the encounter complex, the reaction may proceed. This situation is suggested to correspond to the cases of neutrals **M** = **3**, **4** and **5** for which the overall reaction enthalpy loss is the largest.

Reaction (2) involves a hydrogen atom transfer from the hydroxyl group of ionized carbene **1** to a carbon atom of the neutral molecule **M**. For **M** = **2–5** the ΔH° of reaction (2) is situated between −10 and −30 kJ/mol, these values imply a lower exothermicity than that of reaction (1), nevertheless, m/z 44 ions are almost always detected (Table 1). This difference may be ascribed to differences in the mechanism of the two reactions. If reaction (1) looks like a pure hydrogen atom transfer between two radical sites the situation is different for reaction (2). In the latter case, the reactive step may be visualized by the initial proton transfer of the hydroxylic hydrogen toward the π -electron system of the neutral reactant, followed by a rapid charge exchange. The critical energy for such a reaction is probably less than that associated with a pure free radical process. Another attractive explanation is that m/z 44 ions does not originate from a direct bimolecular event such as reaction (2) but, rather, from a condensation–elimination process as it will be described in Section 3.2.

As expected from the calculated proton affinity value of the radical $(\text{NH}_2\text{CO})^{\bullet}$ (protonation at the oxygen), reaction (3) becomes important only when the proton affinity of **M** is close to or higher than 740 kJ/mol (Table 1). It should be noted however that it is not the major process for most of the studied couples of reactant although proton transfer is known to be a very efficient reaction when its exothermicity is in excess by only a tenth of kJ/mol.

3.2. Condensation processes

Beside hydrogen atom and proton transfers, a large part of the product ions appears to correspond to the loss of a radical, or a molecule, from an elusive adduct

between ion **1** and the molecule M. Table 1 shows that these processes represent up to ~60% of the product ion current at half reaction time. The m/z 72 ions are observed during experiments with ethene, propene and 1-butene, their elemental compositions are $[C_3, N, O, H_6]$. These ions present identical CID spectra dominated by peaks at m/z 55 (50%, NH_3 loss) and 27 (45%, $NH_3 + CO$ loss), a small peak at m/z 44 (5%, C_2H_4 loss) is also observed. Moreover, these spectra are superimposable to that of ions m/z 72 coming from electron ionization of valeramide which have been established to be of protonated acrylamide structure, $[CH_2CHC(OH)NH_2]^+$ [14a]. Loos et al. [14a] showed recently that the metastable ion spectrum of this $[CH_2CHC(OH)NH_2]^+$ structure presents a major peak at m/z 55 and a weak signal at m/z 44. Our CID spectrum presents the same peaks plus the m/z 27 signal pointing to a subsequent elimination of a CO molecule from the acylium ion m/z 55, $[CH_2CHCO]^+$. It may be noted that, as expected, both peaks m/z 55 and m/z 44 appear in high yield in the high energy collisional activation spectrum of protonated acrylamide [13]. Finally, our observation of a small peak at m/z 44 in the low energy CID spectrum of m/z 73 ions with $M = 2$ -butene may be interpreted by a trace of protonated vinylacetamide ions (see below for a discussion concerning the characterization of this structure).

In a similar way, the m/z 86 ions formed by reaction of **1** with 2-butene give CID spectra containing two major signals at m/z 69 (46%, NH_3 loss) and 41 (44%, $NH_3 + CO$ loss) interpretable by the generation, by NH_3 loss, of an acylium ion m/z 69 which in turn expels a molecule of carbon monoxide. A small peak also appears at m/z 44 (10%, $[NH_2CO]^+$ ions). The MIKE spectra of protonated crotylamide, methacrylamide and vinylacetamide have been reported recently [14a]. The former presents only one peak at m/z 69, the second two peaks at m/z 69 (100%) and m/z 58 (23%) and the latter essentially one peak at m/z 43. Since, in our low energy CID spectrum, we observe mainly m/z 69 and its decomposition products one may conclude that the m/z 86 ions produced in our experiments, by reaction of **1** with 2-butene, are principally protonated crotylamide,

$[CH_3CHCHC(OH)NH_2]^+$. When 1-butene is used as neutral reactant the CID spectrum of the m/z 86 product ions is different, it presents four peaks at m/z 69 (10%, NH_3 loss), 44 (42%, $[NH_2CO]^+$ ions), 43 (10%, $HNCO$ loss) and m/z 41 (18%, $NH_3 + CO$ loss), no signal is detected at m/z 58. The most logical explanation of the present results is the existence of a mixture of m/z 86 ions. Protonated crotylamide, $[CH_3CHCHC(OH)NH_2]^+$ would be responsible of the low intensity signals at m/z 69 and 41, while protonated vinylacetamide, $[CH_2CHCH_2C(OH)NH_2]^+$ gives the couple of ions m/z 44 and 43. We note that both ions differ by the attachment of a proton between two bases of similar proton affinities (753.0 and 751.6 kJ/mol for $HNCO$ and propene, respectively [18]). This remark is in line with the MIKE [14a] and high energy CID [13] spectra of protonated vinylacetamide which are dominated by peaks at m/z 43 and 44, respectively.

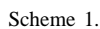
Finally, ions m/z 73 of formula (C_3, H_7, N, O) , formed with 2- and 1-butene were also subjected to collisional experiments. The interpretation of the data are less straightforward since the same peaks are observed in both spectra at m/z 39, 44, 45, 56 and 72. However, significant and reproducible differences in intensities suggest that the two reactions do not lead to the same (mixture of) structure(s). The peaks at m/z 44 ($C_2H_5^\bullet$ loss) and 45 (C_2H_4 loss) are of higher intensity when $M = 1$ -butene, while the H^\bullet and NH_3 losses (m/z 72 and 56) are more intense for $M = 2$ -butene. We tentatively interpret these observations by the formation of a structure more prone to ethene elimination in the former case, i.e., the distonic ion $[CH_2CH_2C(OH)NH_2]^{\bullet+}$. This ion is probably in admixture with the highly stabilized ionized enolamine $[CH_3CHC(OH)NH_2]^{\bullet+}$ ions as it will be discussed in the following section.

Experimental and theoretical results concerning the behavior of the four compounds M of interest in presence of ion **1** are discussed separately in the lines below.

- Reaction between ionized aminohydroxycarbene, **1**, and ethene, **2**, gives mainly rise to ions at

direct hydrogen atom transfer (reaction (2)) or from a loss of an ethyl radical from the $[C_3,N,O,H_7]^{\bullet+}$ adduct. These results lead to the suggestion that the approach of ion **1** toward the ethene molecule gives rise to a covalently bonded species which may further isomerize and dissociate by elimination of H^{\bullet} , $[NH_2]^{\bullet}$ or an ethyl radical. The most simple mechanistic pathway accounting for this scenario is depicted in [Scheme 1](#). It involves the initial formation of the distonic ion $[CH_2CH_2C(OH)NH_2]^{\bullet+}$, **12a**, and its isomerization by H-shifts into ionized propanamide $[CH_3CH_2CONH_2]^{\bullet+}$, **12c**, or ionized enolamine $[CH_3CHC(OH)NH_2]^{\bullet+}$, **12b**. Simple bond cleavages from these three intermediates would lead to the observed fragment ions m/z 72 and m/z 57.

Two kinds of arguments support this proposal: thermochemistry and a comparison with the behavior of ionized aliphatic amides [12–14]. First of all, the



Scheme 1.

energy levels of the dissociation products are obviously below that of the reactants **1**+**2** (see Table A.1 in Appendix A for the various thermochemical data used to comfort Scheme 1). Second, using $\Delta_f H^\circ(\mathbf{12c}) = 658$ kJ/mol, it appears that ionized propanamide **12c** is below the reactants **1**+**2**. Furthermore, it is now well established that, in the carbonyl series, distonic ions and ionized enols are more stable than their carbonylated isomers. For example, in the aldehyde series, the 1,3-distonic ion $[\text{CH}_2\text{CH}_2\text{CHOH}]^{\bullet+}$ and the ionized enol $[\text{CH}_3\text{CHCHOH}]^{\bullet+}$ are more stable than ionized propanal $[\text{CH}_3\text{CH}_2\text{CHO}]^{\bullet+}$ by ~ 50 and ~ 110 kJ/mol, respectively (MP2/6-311+G**//MP2/6-31G* calculations [17]). In a recent thorough investigation of ionized valeramide, it has been found that the

1,3-distonic ion and the ionized enol are more stable than the carbonyl structure by 55 and 80 kJ/mol, respectively (B3LYP/6-311++G**//B3LYP/6-31G* level [14b]). The heats of formation estimated to 625, 560 and 658 kJ/mol for structures **12a–12c** are in line with this general trend. This means that the three intermediates **12a–12c** are below the reactants **1**+**2** by not less than ~ 200 , 270 and 170 kJ/mol, respectively. This large energy gap allows the occurrence of various isomerization reactions such as those presented in Scheme 1, i.e., essentially 1,2- and 1,4-H migrations. Similar reactions have been examined in the case of ionized propanal [17], where it has been shown that the 1,4-H migration $[\text{CH}_3\text{CH}_2\text{CHO}]^{\bullet+} \rightarrow [\text{CH}_2\text{CH}_2\text{CHOH}]^{\bullet+}$ and the

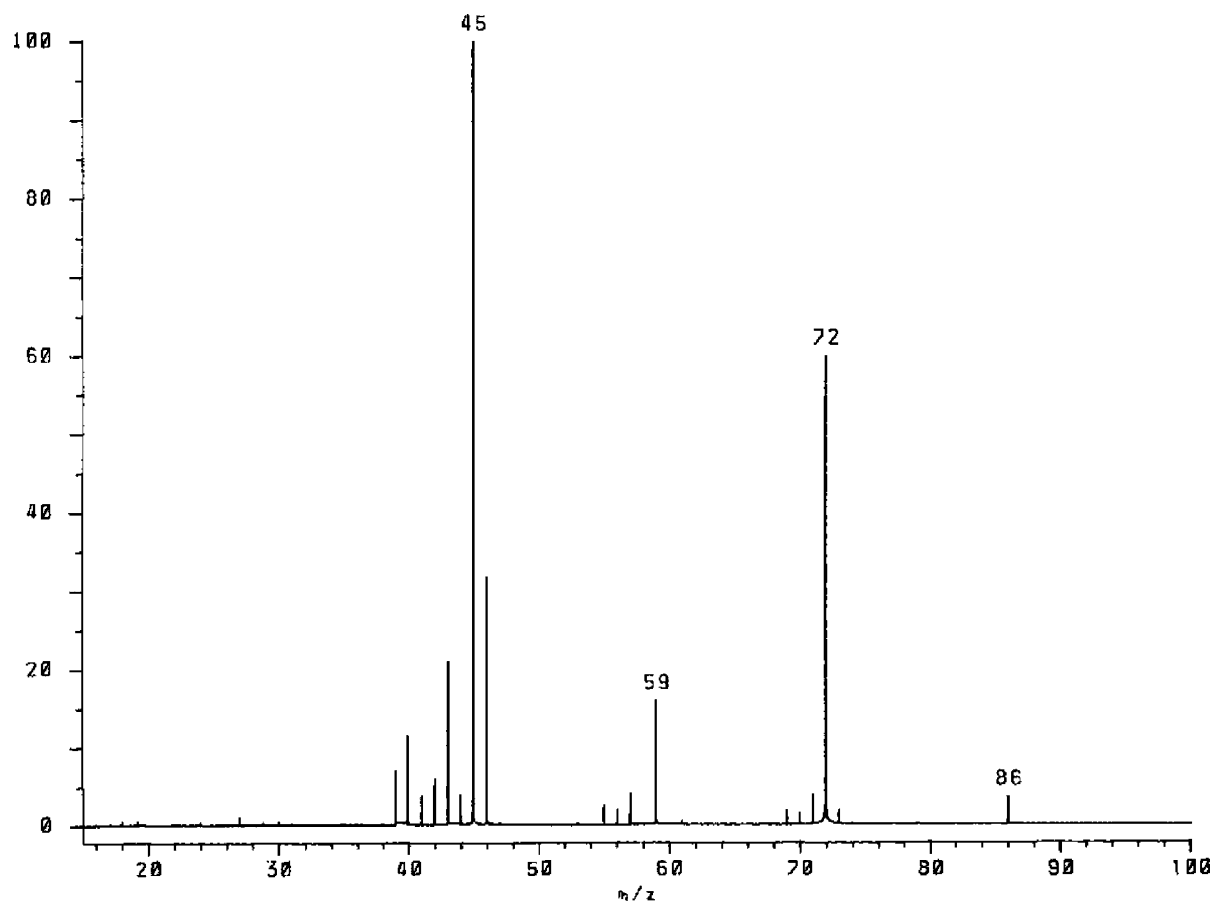


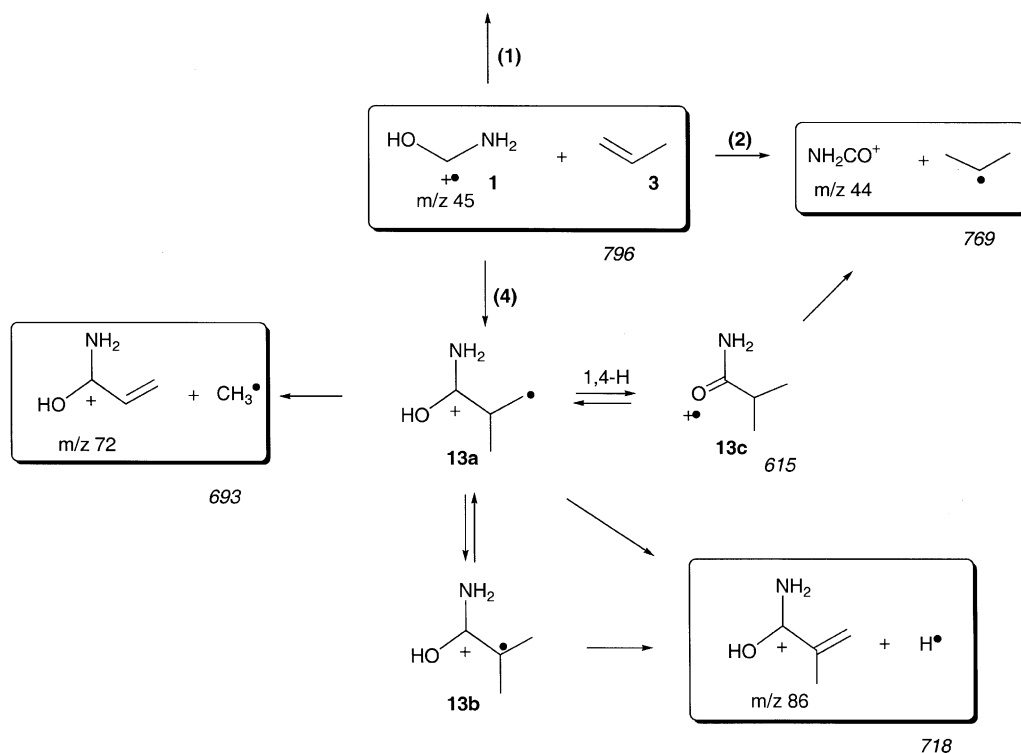
Fig. 2. FT-ICR spectrum for the reaction of **1** with propene **3** ($P = 1.2 \times 10^{-8}$ mbar) after 5 s reaction time.

1,2-H shift $[\text{CH}_2\text{CH}_2\text{CHOH}]^{\bullet+} \rightarrow [\text{CH}_3\text{CHCHOH}]^{\bullet+}$ needs ca. 60 kJ/mol. Assuming similar values in the present case (values in parentheses, Scheme 1), it is clear that transition structures **12ab** and **12ac** are easily accessible from **1** + **2** thus explaining the rapid elimination of H^\bullet or NH_2^\bullet (and probably also, at least for a part, $\text{C}_2\text{H}_5^\bullet$).

It is interesting to note that the low energy–low temperature electron ionization mass spectrum of propanamide presents only two peaks at m/z 73 ($\text{M}^{\bullet+}$) and m/z 72 [12]. According to Scheme 1 this process is indeed the dissociation of lowest energy. As also expected from Scheme 1, the 70 eV mass spectrum present major peaks at m/z 29, 44 and 57 and only a small signal at m/z 72 since the latter process involves a rearrangement and the formers simple bond cleavages. The FT-ICR results presented above show an intermediate figure in accordance with the fact that ion molecule reaction between **1** and **2** results in

ionized propanamide containing 170 kJ/mol of excess energy.

Finally we carried out experiments between **1** and deuterated ethene C_2D_4 in the FT-ICR cell and examined the mass shifts in the high resolution mode. The peak at m/z 57 is mainly shifted to m/z 61 (80%), but small amounts of m/z 60 (15%) and m/z 59 (5%) are however noticeable. The latter signals corresponds to NHD and ND_2 losses and consequently points to a noticeable H/D exchange ($\sim 20\%$) involving the amino group which may occur within the collision complex before the formation of the covalent bond. However, less efficient 1,4-H shifts involving structures **12d** and **12e** (Scheme 1) may also explain these observations. Another possibility is the intermediacy of a sufficiently long lived ion–neutral complex between NH_2 and the acylium ion $[\text{C}_2\text{HD}_4\text{CO}]^+$ which may allow the observed H/D exchange. Concerning the hydrogen atom loss, the two peaks observed at m/z 75 and m/z 76 are



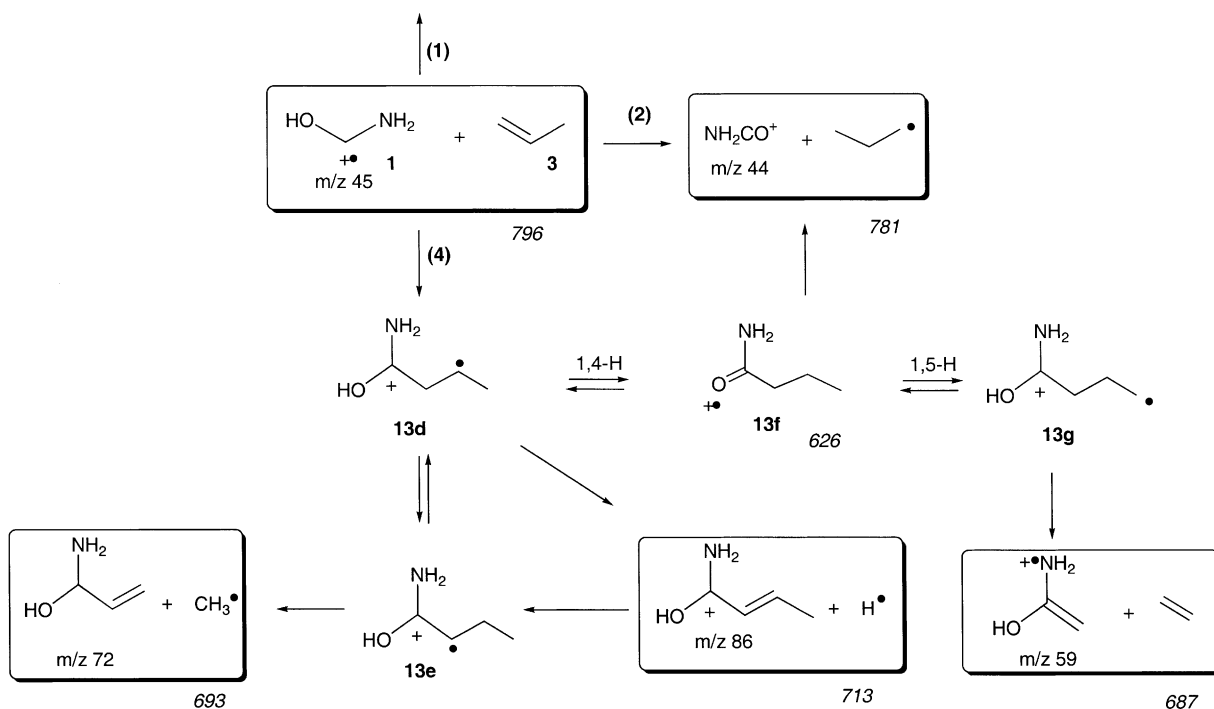
Scheme 2.

in the ratio $\sim 2:1$ indicating, as expected, a preferred elimination of a deuterium atom. However, since the deuterium loss is probably attenuated by an isotope effect, no conclusion can be drawn concerning the extent of the H/D exchange preceding this reaction. Finally, we note that m/z 44, $[\text{NH}_2\text{CO}]^+$, and m/z 45, $[\text{NH}_2\text{COH}]^+$, ions do not incorporate any deuterium atom to a detectable level and that no m/z 46 ions are observed, even at reaction time as long as 30 s. It may thus be concluded that a large part of m/z 44 ions probably occur from the direct hydrogen abstraction reaction (2) rather than from dissociation of the intermediate **12c**.

- Propene, **3**, reacts with **1** mainly via the condensation route, the major peak observed at m/z 72 corresponds to the loss of a methyl radical from the adduct **1** + **3** (Fig. 2). As noted above, the CID spectrum of these ions demonstrates that they are of protonated acrylamide structure. As attested by high resolution measurements, the ions m/z 59 are

of formula $[\text{C}_2\text{O}_2\text{N}_2\text{H}_5]^+$ and consequently originate from an ethene elimination from the adduct. A minor signal corresponding to the elimination of H^\bullet (m/z 86) from the adduct **1** + **3** is also noticeable. By contrast with the ethene case, no m/z 44 ions have been detected in our experiments with propene.

Again the results may be explained by the initial formation of a covalent bond in the adducts, the situation is however complicated here by the fact that the two unsaturated carbon atoms of the neutral reactant, **3**, are not identical. For the sake of clarity, two schemes were drawn in order to illustrate the two modes of approach of ion **1** toward **3** (Schemes 2 and 3). Electrophilic attack of **1** on the central carbon of neutral propene, **3**, leads to the distonic ion **13a** which may isomerize to ionized enolamine **13b** or ionized 2-methyl propanamide **13c** (Scheme 2). Simple cleavages from these ions would produce m/z 86, 72 and 44. In a similar way, the approach of **1** toward the carbon atom of the methylene group of **3**, may



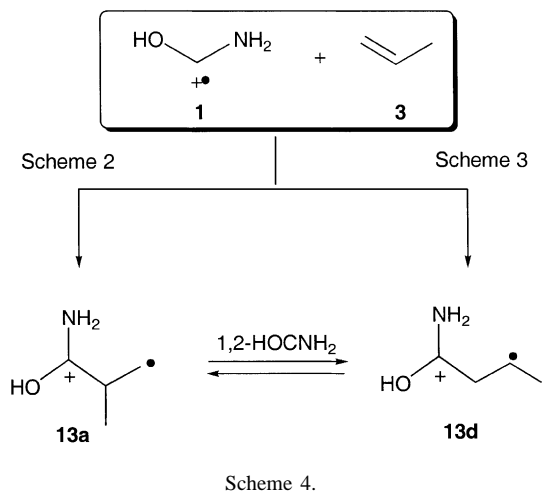
Scheme 3.

give rise to the species **13d–13g**, the latter being the precursor of ions m/z 59 (Scheme 3).

The validity of these proposals is first supported by the favorable exothermicity of the overall processes. Accordingly, the products enthalpies of formation corresponding to ions m/z 86, 72 and 59 are below **1** + **3** by ca. 80 to 110 kJ/mol. Considering that the carbonylated covalent forms **13c** and **13f** are more stable than **1** + **3** by 170–180 kJ/mol it is evident that they are able to isomerize via the elementary steps depicted in Schemes 2 and 3. It is also noteworthy that no significant signal at m/z 71 (NH_2^\bullet loss from **13c** or **13f**) has been detected during the experiments thus indicating that all the observed chemistry occurs more readily than direct bond cleavages leading to final products at an enthalpy level situated around 769–781 kJ/mol.

The observation of a significant peak at m/z 59 indicates that the reactions presented in Scheme 3 are operational. It does not mean however that the reactions of Scheme 2 are inoperative since it is probable that **1** approaches **3** at one or the other side of the CC double bond (i.e., a 100% regioselectivity is unlikely). A way to distinguish between the two routes would be to check the structure of the m/z 86 ions. Unfortunately the corresponding peak intensity is too low to allow, for example, collision experiment in the FT-ICR cell. Moreover, even if a 100% regioselectivity is operative, an overlap between the mechanistic steps presented in Schemes 2 and 3, achieved for example via a 1,2- OHCNH_2 shift, as sketched in Scheme 4, cannot be excluded.

In this context, it is interesting to compare the above described experimental results to the MIKE spectra of ionized butanamide and ionized 2-methylpropanamide. Both spectra exhibit an intense peak at m/z 59 (ethene loss) and two signals at m/z 70 (NH_3 loss) and m/z 72 (CH_3^\bullet loss). It is quite remarkable that the relative peak intensities are identical in both spectra (100, 6 and 20%, respectively). One may also recall that the low energy–low temperature electron ionization mass spectra of butanamide and 2-methylpropanamide are dominated by the peak at m/z 59 [12]. Thus, the most favorable dissociation



pathway from the two molecular ions **13c** and **13f** is the ethene loss which is best described by the McLafferty rearrangement involving the 1,5-hydrogen migration **13f** → **13g**. Ethene elimination from **13c** needs a skeletal rearrangement of the isopropyl chain which, obviously, may be achieved by the 1,2- HOCNH_2 shift **13a** → **13d** presented in Scheme 4. The 1,4-hydrogen transfers **13f** → **13d** and **13c** → **13a** complete the connection between ionized butanamide, **13f**, and ionized 2-methylpropanamide, **13c**. Reaction **13f** → **13g** → m/z 59 + C_2H_4 is expected to occur at its thermochemical threshold since the products are situated 60 kJ/mol above **13f**. This is largely enough to overcome the 1,5-hydrogen migration barrier. The fact that the MIKE spectra of **13c** is identical to that of **13f** means that the 1,4-hydrogen transfers **13f** → **13d** and **13c** → **13a** and the 1,2- HOCNH_2 shift **13a** → **13d** also occur below the energy level of the products of the McLafferty rearrangement. Finally, one can observe that the ratio of peak intensities m/z 59/ m/z 72 is equal to five from the MIKE spectra of butanamide and 2-methylpropanamide, but is less than unity from the ion–molecule reaction between **1** and **3** in the FT-ICR experiments. This is so because, in the latter case, the system is sampled at a higher internal energy thus favoring the methyl loss which may occur directly from the initial adduct **13a**.

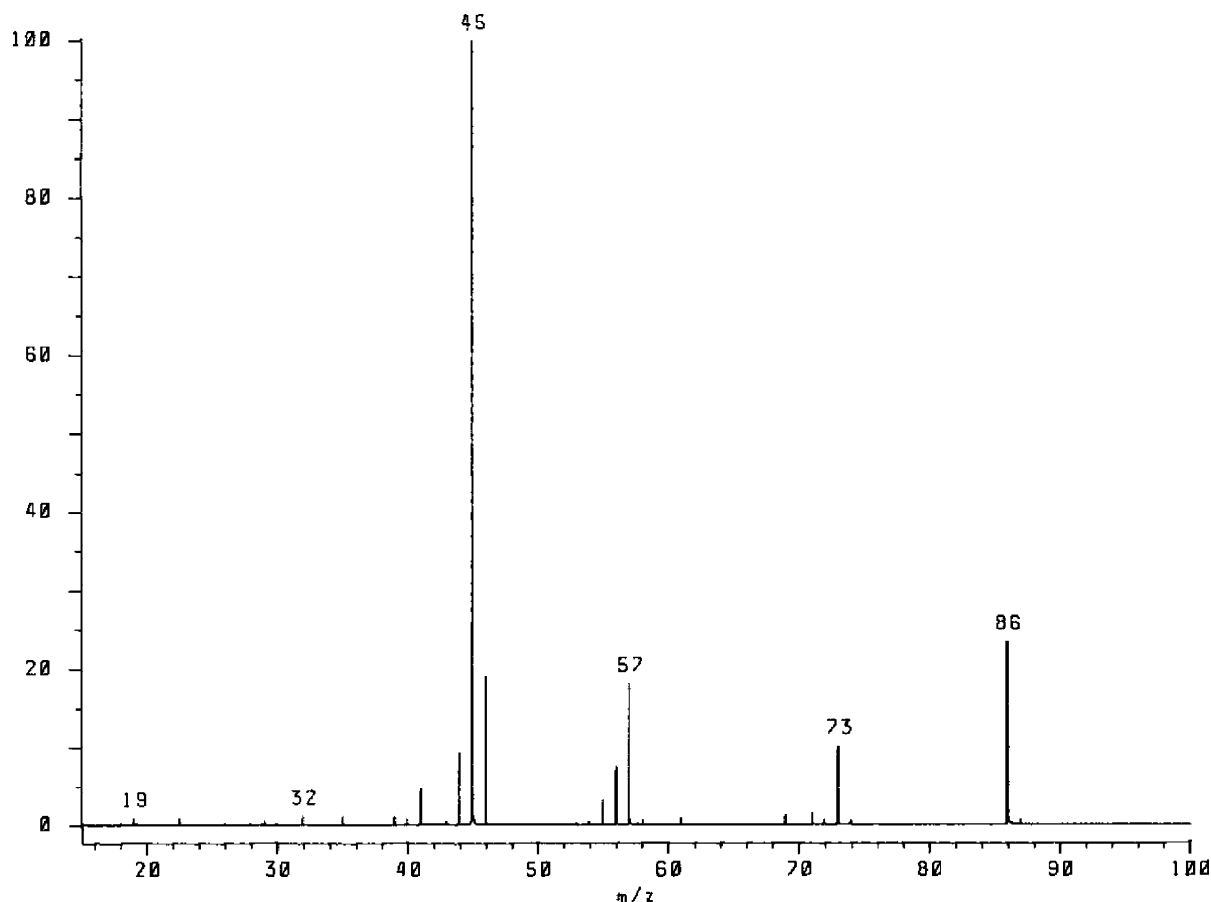


Fig. 3. FT-ICR spectrum for the reaction of **1** with 2-butene **4** ($P = 1.1 \times 10^{-8}$ mbar) after 3.5 s reaction time.

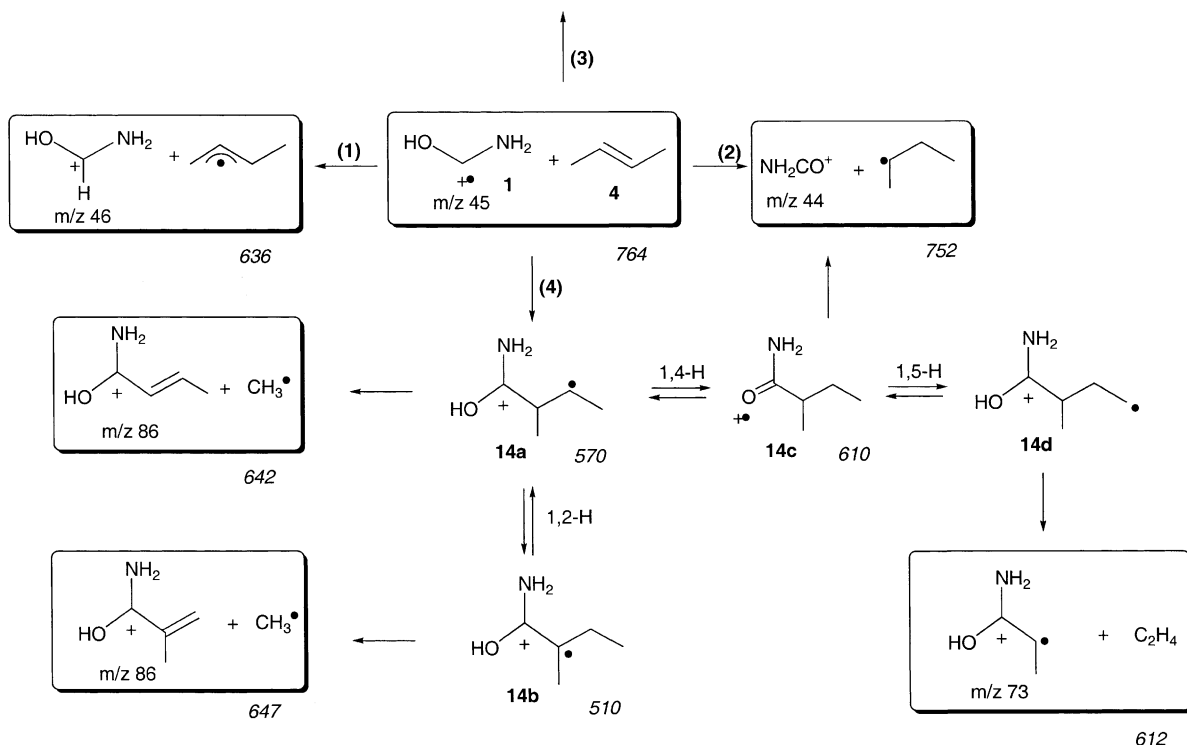
- Reaction of **1** with 2-butene, **4**, produces two significant ions at m/z 86 (CH_3^\bullet loss) and m/z 73 (C_2H_4 loss) of structures $[\text{CH}_3\text{CHCHC}(\text{OH})\text{NH}_2]^+$ and (probably) $[\text{CH}_3\text{CHC}(\text{OH})\text{NH}_2]^+$, as established from CID experiments (Fig. 3).

A, now familiar, mechanistic scheme is proposed in order to explain the experimental observations (Scheme 5). Again, the initial formation of a 1,3-distonic ion, **14a**, is the starting point of the various isomerization–dissociation steps.

Structure **14a** is the direct precursor of the m/z 86, $[\text{CH}_3\text{CHCHC}(\text{OH})\text{NH}_2]^+$ ions produced by methyl loss. It may be recalled that the isomeric ion, protonated methacrylamide, $[\text{CH}_2\text{C}(\text{CH}_3)\text{C}(\text{OH})\text{NH}_2]^+$,

has not been evidenced from the CID spectrum of the m/z 86 ions produced by reaction of **1** with 2-butene. This is in keeping with a slightly higher heat of formation of the latter but is more probably due to the slowdown effect of the formation of the highly stable isomeric ion **14b**. According to the reaction scheme, the most likely m/z 73 candidate structure is ionized enolamine $[\text{CH}_3\text{CHC}(\text{OH})\text{NH}_2]^+$. The lower intensity of the peak m/z 73, whereas the enthalpy of the products is lower than that of the m/z 86 ion, is probably illustrative of the non-negligible critical energy of the 1,4-hydrogen atom migration **14a** \rightarrow **14c**.

The limited number of condensation products from the **1** + **4** reactants is at variance from that of the isomeric system **1** + **5** suggesting inefficient



Scheme 5.

connection between them, as discussed in the following section.

- The case of 1-butene, **5**, like that of propene, **3**, presents the possibility of a double approach of the ionized reactant **1** toward the CC double bond. Four product ions are detected at m/z 86 (CH_3^\bullet loss), 73 (C_2H_4 loss), 72 ($\text{C}_2\text{H}_5^\bullet$ loss) and m/z 59 (C_3H_6 loss) (Fig. 4). In the section devoted to the description of the CID results it has been concluded that m/z 86 ions are a mixture of $[\text{CH}_3\text{CHCHC}(\text{OH})\text{NH}_2]^+$ and $[\text{CH}_2\text{CHCH}_2\text{C}(\text{OH})\text{NH}_2]^+$ structures and that m/z 72 are, unambiguously, $[\text{CH}_2\text{CHC}(\text{OH})\text{NH}_2]^+$ ions. Concerning m/z 73 ions the possible formation of a mixture of $[\text{CH}_2\text{CH}_2\text{C}(\text{OH})\text{NH}_2]^\bullet+$ and $[\text{CH}_3\text{CHC}(\text{OH})\text{NH}_2]^\bullet+$ structures has been tentatively suggested. The intensity of the m/z 59 peak was too low to allow CID experiments to be made, it is however highly probable that it is ionized enamine $[\text{CH}_2\text{C}(\text{OH})\text{NH}_2]^\bullet+$ since it is the most sta-

ble structure corresponding to this CCON frame and the most logical product for an elimination of a propene molecule in the present system.

The two distonic structures expected to be initially produced, **15a** and **15e** (Scheme 6), are the entry points for the isomerization paths of ionized valeramide (Scheme 7) and 2-methyl butanamide (already considered in Scheme 5). Also indicated in Scheme 6, is the possibility of a 1,2-HOCNH₂ shift connecting **15a** and **15e**.

The difference observed between 2- and 1-butene in their reactions with **1**, in particular the formation of ions m/z 72 and m/z 59 and the differences in structures for ions m/z 73 and 86, suggest that the mechanistic pathways depicted in Scheme 5, alone, cannot explain the behavior of 1-butene.

Following Scheme 6, the attack of **1** on the carbon C₍₂₎ of the molecule of 1-butene gives rise to **15e** which may lead directly to the ions m/z 72 by

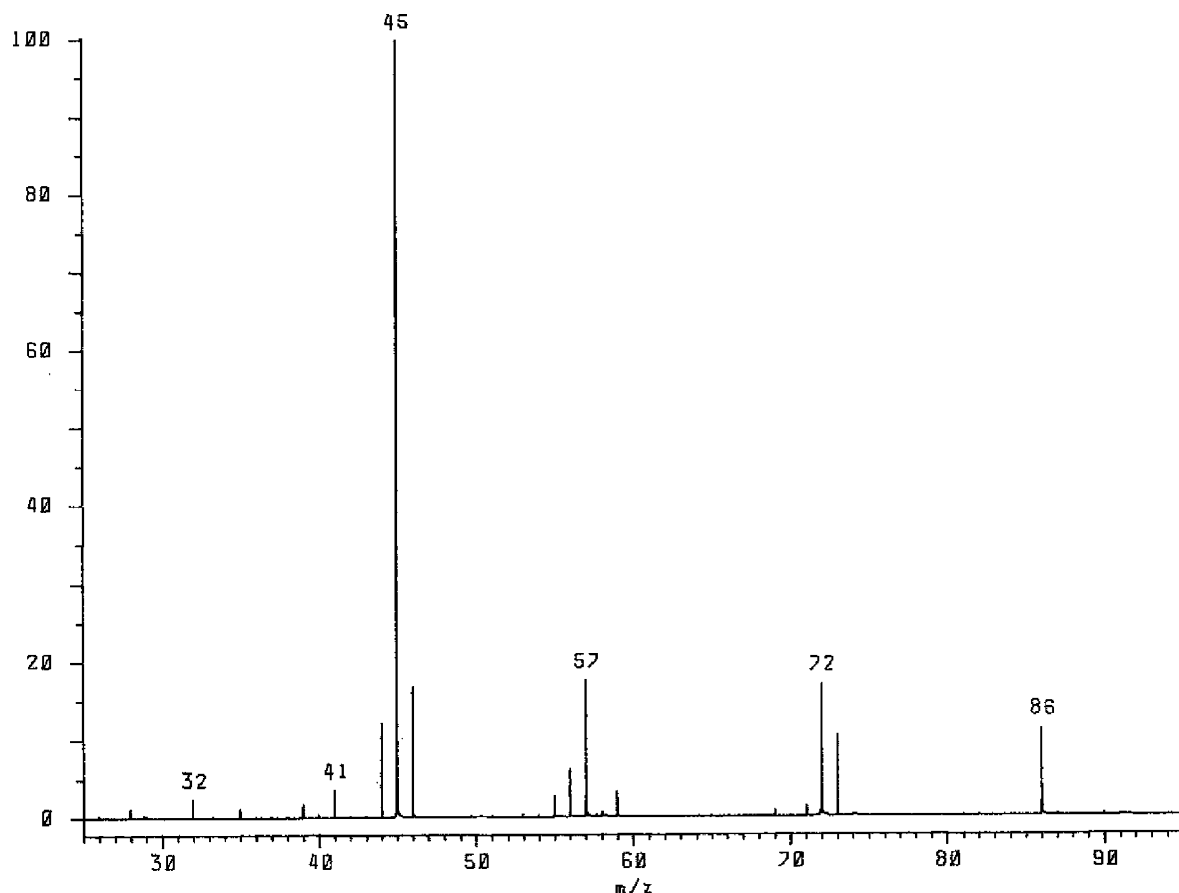
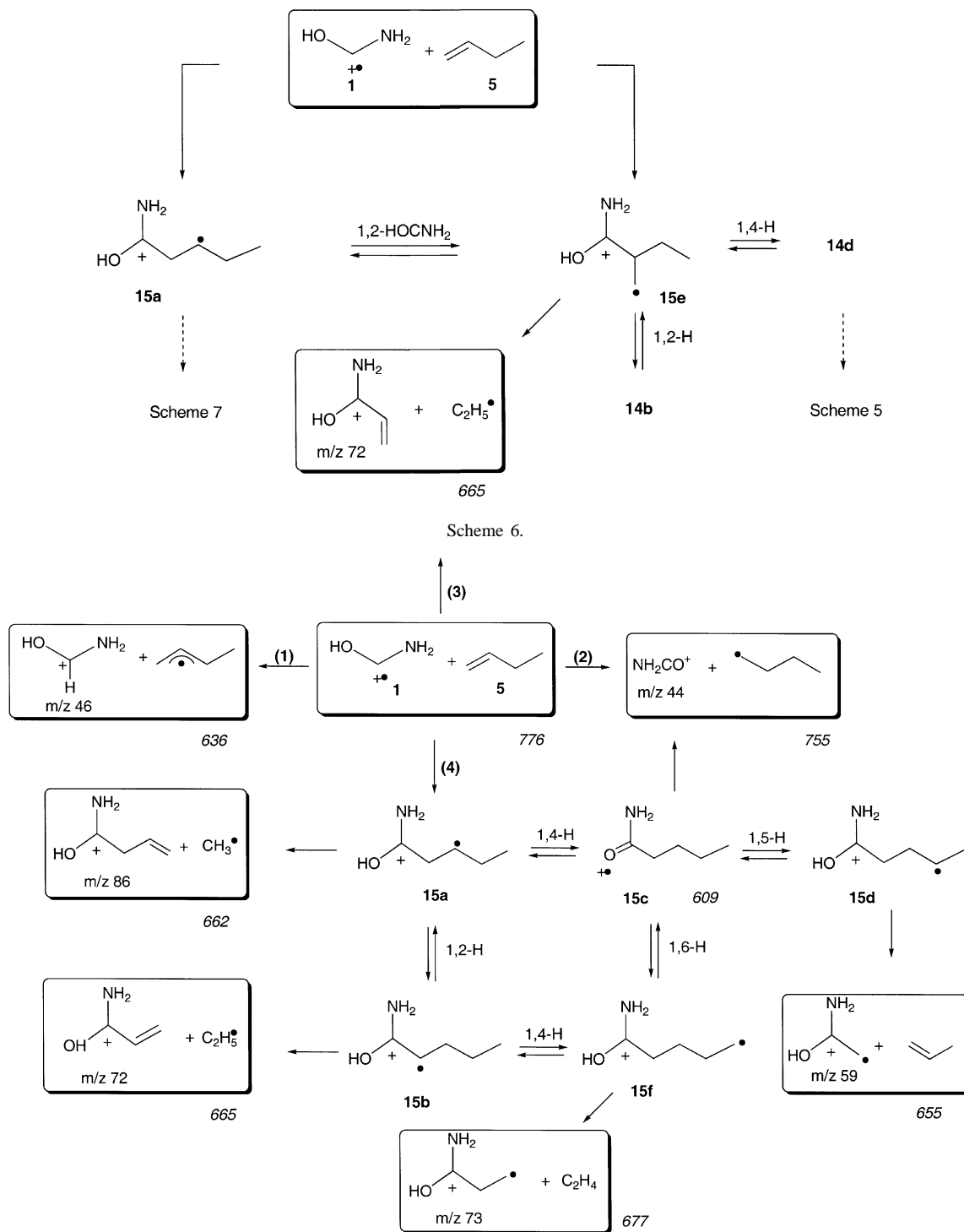


Fig. 4. FT-ICR spectrum for the reaction of **1** with 1-butene **5** ($P = 1.0 \times 10^{-8}$ mbar) after 5 s reaction time.

ethyl loss. Accordingly, this is the major dissociation path for reaction of **1** with 1-butene, it was not observed with the 2-butene. Isomerization by a 1,4-hydrogen migration **15e** \rightarrow **14d** produces the 1,4-distonic structure which may be at the origin of the $[\text{CH}_3\text{CHC}(\text{OH})\text{NH}_2]^{\bullet+}$ ions. All the other peaks would necessarily arise from structure **15a** produced either by the attack of **1** on the carbon $\text{C}_{(1)}$ of the molecule of 1-butene, or from the 1,2-HOCNH₂ migration **15e** \rightarrow **15a**. Thus, let us look at Scheme 7, which illustrates the evolution of the system starting from **15a**. Isomerization of this 1,3-distonic ion into ionized valeramide **15c** explains the formation of ions m/z 59 via a McLafferty rearrangement involving the intermediate **15d**. In competition with the

1,5-hydrogen migration **15c** \rightarrow **15d**, the 1,6-hydrogen transfer **15c** \rightarrow **15f** opens the possibility of formation of the distonic ion m/z 73, $[\text{CH}_2\text{CH}_2\text{C}(\text{OH})\text{NH}_2]^{\bullet+}$ by ethene elimination. The second possible isomerization route from the 1,3-distonic adduct **15a** is the 1,2-hydrogen shift **15a** \rightarrow **15b**, it offers another way to produce m/z 72 ions, $[\text{CH}_2\text{CHC}(\text{OH})\text{NH}_2]^+$, by loss of an ethyl radical. Finally the direct elimination of a methyl radical from the ion **15a** may produce m/z 86 ions of protonated vinylacetamide structure. At this stage it is comforting to observe that our FT-ICR results are formally comparable to that obtained during the study of the unimolecular chemistry of ionized hexanamide [13] and valeramide [14]. Moreover, several of the mechanistic steps



Scheme 7.

presented in Schemes 5–7 have been recently subjected to molecular orbital calculations [14b]. Fortunately, all the transition structures are predicted to be significantly below the energy level of the reactants **1** + 1- or 2-butene, thus giving weight to the mechanistic proposals depicted in Schemes 5–7.

4. Conclusion

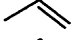

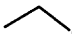

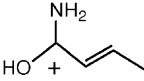
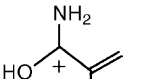

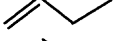

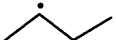

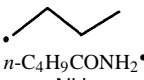
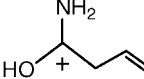
The bimolecular reactivity of ionized aminohydroxycarbene $[\text{NH}_2\text{COH}]^{\bullet+}$, **1**, toward the simplest alkenes offers a large palette of the radical-cation/neutral chemistry. The compound **1** may act as a H atom acceptor or a H atom donor. The former reaction is associated with a large energy barrier indicative of a pure hydrogen atom transfer. The latter appears to have a lower energy barrier suggesting another type of reaction. The proton affinity of the radical $\text{NH}_2\text{CO}^{\bullet}$ is calculated to be 740 kJ/mol at the G2 level, this is corroborated by the observation of a limited proton transfer with ethene, propene and butenes which offer a 680–752 kJ/mol proton affinity range.

The most significant finding is the condensation reaction which may be considered as another example of charge catalyzed free radical addition on the CC double bond. These reactions constitute moderate energy entry points in the potential energy surface of ionized amides.

Table A.1
Heats of formation (kJ/mol) of the various species considered

Species	$\Delta_f H_{298\text{ K}}$	Method (reference)
$\text{NH}_2\text{C}^{\bullet+}\text{OH}$	776	G2
$\text{NH}_2\text{CH}^+\text{OH}$	503	G2
$\text{NH}_2\text{C}^+\text{O}$	681	G2
$\text{NH}_2\text{C}^{\bullet}\text{O}$	–14	G2
C_2H_4	52	[19]
$\text{C}_2\text{H}_3^{\bullet}$	265	[19]
C_2H_5^+	902	[19]
$\text{C}_2\text{H}_5^{\bullet}$	119	[20]
H^{\bullet}	218	[19]
NH_2^{\bullet}	189	[19]
$\text{C}_2\text{H}_5\text{CONH}_2^{\bullet+}$	658	[19]
$\text{C}_2\text{H}_5\text{CO}^+$	591	[19]

Table A.1 (Continued)

Species	$\Delta_f H_{298\text{ K}}$	Method (reference)
$\text{CH}_2=\text{CHC}^+(\text{OH})\text{NH}_2$	516	G2
$\text{CH}_2=\text{C}(\text{OH})\text{NH}_2^{\bullet+}$	635	G2
CH_3^{\bullet}	147	[19]
$n\text{-C}_3\text{H}_7\text{CONH}_2^{\bullet+}$	626	– ^a
$i\text{-C}_3\text{H}_7\text{CONH}_2^{\bullet+}$	615	– ^b
$n\text{-C}_3\text{H}_7\text{CO}^+$	562	[19]
$i\text{-C}_3\text{H}_7\text{CO}^+$	548	[19]
	20	[19]
	88	[20]
	100	[20]
	171	[20]
	495	– ^c
	500	– ^d
	0	[19]
	–12	[19]
	69	[20]
	133	[19]
	74	[19]
$n\text{-C}_4\text{H}_9\text{CONH}_2^{\bullet+}$	609	[14b]
	515	[14b]
	625	[14b]

^aFrom $\Delta_f H_{298\text{ K}}$ (neutral) = –279 kJ/mol [19] and an adiabatic ionization energy of 9.38 eV assumed to be identical to that of 2-pentanone [19].

^bFrom $\Delta_f H_{298\text{ K}}$ (neutral) = –283 kJ/mol [19] and an adiabatic ionization energy of 9.30 eV assumed to be identical to that of 2-methylbutanone [19].

^cFrom $\Delta_f H_{298\text{ K}}$ $[\text{CH}_2=\text{CHC}(\text{OH})\text{NH}_2]^+ = 546$ kJ/mol (G2 calculation) and corrected for the methyl substitution by considering the heats of formation of the homolog ions $[\text{CH}_2=\text{CHCH}(\text{OH})]^+$ and $[\text{CH}_3\text{CH}=\text{CHCH}(\text{OH})]^+$ (642 and 591, respectively) [19].

^dFrom $\Delta_f H_{298\text{ K}}$ $[\text{CH}_2=\text{CHC}(\text{OH})\text{NH}_2]^+ = 546$ kJ/mol (G2 calculation) and corrected for the methyl substitution by considering the heats of formation of the homolog ions $[\text{CH}_2=\text{CHCH}(\text{OH})]^+$ and $[\text{CH}_2=\text{C}(\text{CH}_3)\text{CH}(\text{OH})]^+$ (642 and 596, respectively) [19].

Appendix A

Table A.1 contains the heat of formation values, of experimental and theoretical origin, used to support the mechanisms described in **Schemes 1–7**.

References

- [1] Y. Hoppilliard, G. Bouchoux, P. Jaudon, *Nouv. J. Chim.* 6 (1982) 43.
- [2] (a) G. Bouchoux, J.-P. Flammang, Y. Hoppilliard, *Int. J. Mass Spectrom.* 57 (1984) 179;
(b) Y. Apeloig, M. Karni, B. Ciommer, G. Depke, G. Frenking, S. Meyn, J. Schmidt, H. Schwarz, *Int. J. Mass Spectrom.* 59 (1984) 21;
(c) W. Bertrand, G. Bouchoux, *Rapid Commun. Mass Spectrom.* 12 (1998) 1697.
- [3] R. Flammang, M.T. Nguyen, G. Bouchoux, P. Gerbaux, *Int. J. Mass Spectrom.* 202 (2000) 8.
- [4] G. Bouchoux, A. Espagne, *Chem. Phys. Lett.* 348 (2001) 329.
- [5] (a) C.E.C.A. Hop, H. Chen, P.J.A. Ruttink, J.L. Holmes, *Org. Mass Spectrom.* 26 (1991) 679;
(b) G.A. McGibbon, P.C. Burgers, J.K. Terlouw, *Int. J. Mass Spectrom. Ion Process.* 136 (1994) 191;
(c) P.J.A. Ruttink, P.C. Burgers, J.K. Terlouw, *Int. J. Mass Spectrom. Ion Process.* 145 (1995) 35.
- [6] P. Kofel, M. Alleman, H.P. Kelerhals, K.P. Wanczek, *Int. J. Mass Spectrom. Ion Process.* 65 (1985) 97.
- [7] T. Su, W. Chesnavich, *J. Chem. Phys.* 76 (1982) 5183.
- [8] M.J. Frisch, G.W. Trucks, H.B. Schlegel, G.E. Scuseria, M.A. Robb, J.R. Cheeseman, V.G. Zakrzewski, J.A. Montgomery Jr., R.E. Stratmann, J.C. Burant, S. Dapprich, J.M. Millam, A.D. Daniels, K.N. Kudin, M.C. Strain, O. Farkas, J. Tomasi, V. Barone, M. Cossi, R. Cammi, B. Mennucci, C. Pomelli, C. Adamo, S. Clifford, J. Ochterski, G.A. Petersson, P.Y. Ayala, Q. Cui, K. Morokuma, D.K. Malick, A.D. Rabuck, K. Raghavachari, J.B. Foresman, J. Cioslowski, J.V. Ortiz, B.B. Stefanov, G. Liu, A. Liashenko, P. Piskorz, I. Komaromi, R. Gomperts, R.L. Martin, D.J. Fox, T. Keith, M.A. Al-Laham, C.Y. Peng, A. Nanayakkara, C. Gonzalez, M. Challacombe, P.M.W. Gill, B. Johnson, W. Chen, M.W. Wong, J.L. Andres, C. Gonzalez, M. Head-Gordon, E.S. Replogle, J.A. Pople, *Gaussian 98*, Revision A.6, Gaussian Inc., Pittsburgh, PA, 1998.
- [9] L.A. Curtiss, K. Raghavachari, P.C. Redfern, J.A. Pople, *J. Chem. Phys.* 106 (1997) 1063.
- [10] L.A. Curtiss, P.C. Redfern, B.J. Smith, L. Radom, *J. Chem. Phys.* 104 (1996) 5148.
- [11] A. Nicolaides, A. Rauk, M.N. Glukhovtsev, L. Radom, *J. Phys. Chem.* 100 (1996) 17460.
- [12] M. Abebe, A. Maccoll, R.D. Bowen, *Eur. J. Mass Spectrom.* 3 (1997) 197.
- [13] D. Kreft, H.-F. Grutzmacher, *Eur. J. Mass Spectrom.* 4 (1998) 63.
- [14] (a) J. Loos, D. Schröder, W. Zummack, H. Schwarz, R. Thissen, O. Dutuit, *Int. J. Mass Spectrom.* 214 (2002) 105;
(b) M. Semialjac, J. Loos, D. Schröder, H. Schwarz, *Int. J. Mass Spectrom.* 214 (2002) 129;
(c) D. Schröder, J. Loos, M. Semialjac, T. Weiske, H. Schwarz, G. Höne, R. Thissen, O. Dutuit, *Int. J. Mass Spectrom.* 214 (2002) 155.
- [15] (a) R.P. Bell, *Proc. Roy. Soc. London A154* (1936) 414;
(b) M.G. Evans, M. Polanyi, *Trans. Faraday Soc.* 32 (1936) 1333.
- [16] D.M. Camaioni, S.T. Autrey, T.B. Salinas, J.A. Franz, *J. Am. Chem. Soc.* 118 (1996) 2013.
- [17] G. Bouchoux, A. Luna, J. Tortajada, *Int. J. Mass Spectrom. Ion Process.* 167/168 (1997) 353.
- [18] E.P.L. Hunter, S.G. Lias, *J. Phys. Chem. Ref. Data* 27 (1998) 413.
- [19] S.G. Lias, J.E. Bartmess, in: W.G. Mallard, P.J. Linstrom (Eds.), *NIST Chemistry Webbook, NIST Standard Reference Database No. 69*, National Institute of Standards and Technology, Gaithersburg, MD, 2000 (<http://webbook.nist.gov>).
- [20] W. Tsang, in: J.A.M. Simoes, A. Greenberg, J.F. Liebman (Eds.), *Energetics of Organic Free Radicals*, Blakie Academic, London, 1996.